Soft Matter

www.rsc.org/softmatter

Volume 7 | Number 8 | 21 April 2011 | Pages 3653–4072

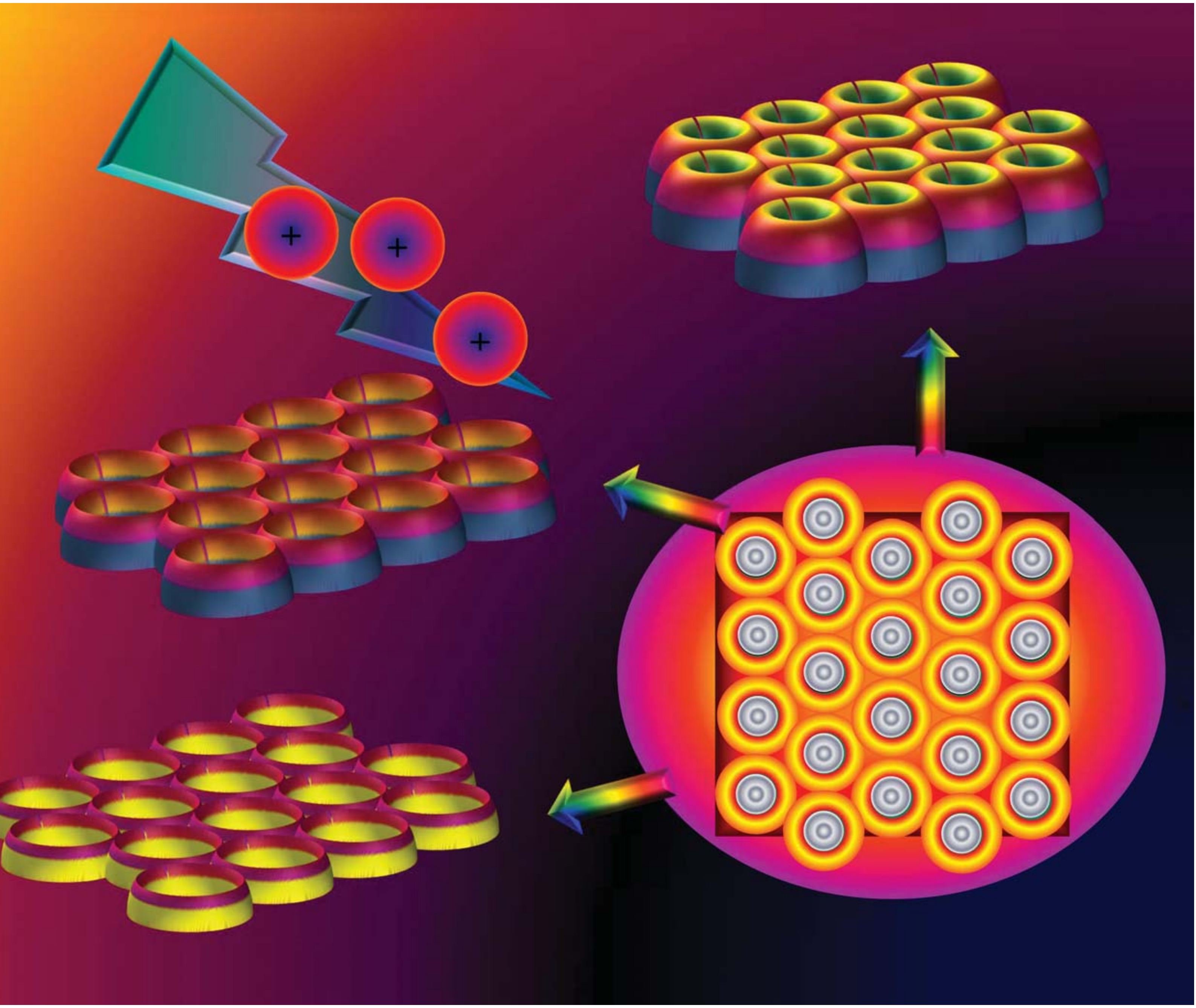

ISSN 1744-683X

RSC Publishing

PAPER

Advincula *et al.*

Non-lithographic electrochemical patterning of polypyrrole arrays using single-layered colloidal templates on HOPG surface: effects of electrodeposition time and field-gradient

Non-lithographic electrochemical patterning of polypyrrole arrays using single-layered colloidal templates on HOPG surface: effects of electrodeposition time and field-gradient†

Jin Young Park,‡ Pampa Dutta and Rigoberto Advincula*

Received 3rd September 2010, Accepted 10th November 2010
DOI: 10.1039/c0sm00926a

Highly ordered conducting polypyrrole sub-micropore arrays were formed on HOPG substrates using the single-layer non-lithographic colloidal templating technique and electrodeposition method. The morphology and the opening sizes on the sub-micropores were highly dependent on the electrodeposition time and thickness. Various shapes of the polymeric arrays were observed including: honeycombs, flat ring-shape, and hollow shells—which can appear on the same sample surface due to gradients on the electrical charge (or distance) passed through a conducting sample.

Introduction

The microfabrication of two-/three-dimensional (2-D/3-D) colloidal particle arrays is of high interest due to their various applications in lithography, optical sensors, photonic band gap devices, and photonic crystals.[1] For these well-ordered colloidal arrays, various arraying methods have been attempted, such as vertical lifting deposition,[2] template-assisted direct self-assembly,[3] electrophoretic deposition,[4] convective self-assembly,[5] evaporation method,[6] and the flow cell methods.[7] In particular, 2-D array films by a Langmuir–Blodgett (LB)-like technique from the air–liquid interface[8] are considered to be effective for monolayer fabrication. With this air–liquid interface method,[9] colloidal particles dispersed with a spreading agent (surfactant) spontaneously form 2-D aggregates at the interface by attractive hydrophobic interactions among the particles. This 2-D array can then be transferred onto the surface of a solid substrate. From this method, it has been possible to form hexagonally packed 2-D singe-layer arrays of colloidal spheres depending on the surfactant concentration and its interaction with the charged polystyrene (PS) particles.

Recently, a considerable interest has been generated on the micro/macropore formation of inorganic materials,[10] metals (Au, Ag, and Pt)[11] or conductive polymeric materials[12] on interstitial voids using the 3-D colloidal array templates. This template-directed method can give well-ordered porous materials with parameter control of the fabrication process. Polypyrrole (Ppy), one of the more well-known conducting polymer materials with stable chemical/physical, biocompatibility, and high electrical conductivity, has been used for constructing 3-D microporous structure. For example, Sumida *et al.* have suggested that well-ordered 3-D porous Ppy array films can be formed by electrochemical oxidation in the presence of ordered arrays of silica spheres as templates.[13] Using 3-D silica templates, porous systems have been demonstrated with different holes sizes, controlled by changing the polymerization potential. Moreover, based on the potentiostatic method, Bartlett *et al.* demonstrated that various conducting polymeric materials can be grown on interstitial voids of the highly ordered 3-D microporous templates.[12a] The immobilization of glucose oxidase (GOx) on a porous Ppy film was suggested to increase the sensing ability in a blood sugar sensor.[14] However, there are only a few research reports on the use of single-layer 2-D colloidal templated films for unconventional applications; for example, development of functional porous membrane films or biosensing elements *via* molecular imprinting techniques. It should be noted that 3-D colloidal templating, while highly applied for photonic applications (inverse opals) or in membrane separations, has great potential for non-lithographic 2-D patterning as *single layers*. To further explore possible applications as single layers, we hereby describe the preparation and investigation of highly ordered 2-D arrays of conducting polymers on highly oriented pyrolytic graphite (HOPG) substrate/electrode using a polystyrene microbead (PS-m) templating technique and the potentiostatic electropolymerization method.

Experimental

Materials

Polystyrene latex beads (0.5 μm in diameter, 2.5% solids (w/v) aqueous suspension, 3.64×10^{11} particles per ml) were purchased from Polyscience Corp. and used without any further purification. These particles contain a slight anionic charge from the sulfate ester. A sodium *n*-dodecylsulfate (SDS) spreading agent was added on the diluted PS-m suspension solution to facilitate the array formation at the air–water interface. Millipore quality water (18 MΩ cm) was added to control the total concentration. Pyrrole (py) and pyrrole 2-carboxaldehyde (py–CHO) from Aldrich were used for electropolymerization on the PS-m array film, and toluene (analytical grade) was used to dissolve (etch out) the PS-m particle arrays.

Department of Chemistry and Department of Chemical and Biomolecular Engineering, University of Houston, Houston, TX, 77204, USA. E-mail: radvincula@uh.edu; Fax: +1-713-743-2709; Tel: +1-713-743-1760

† Electronic supplementary information (ESI) available: This shows the fabrication of the particles using 100 nm templates. See DOI: 10.1039/c0sm00926a

‡ Current address: Department of Polymer Science and Engineering, University of Massachusetts, 120 Governors Drive, Amherst, MA 01003, USA.

PS latex beads array (using LB-like technique)

To fabricate 2-D particle single layer arrays, an LB-like colloidal layering technique was used.[15] This technique can be utilized with no floating barriers. Firstly, the mixture with the concentration of latex particles (1 wt%) and the spreading agent (sodium *n*-dodecylsulfate, SDS) in the range of 34.7 mM for SDS was prepared. On the basis of the fixed latex concentration and the surface area of 0.5 μm sphere, the saturation concentration of the surfactant on the latex surface was estimated to be sufficiently low.[15] The dispersion was sonicated for 10–15 min prior to transfer on the substrate. Instead of a conventional trough, a glass cylinder (15 mm in diameter–25 mm in height) was used. The dispersion with PS-m and the spreading agent was filled in the glass cylinder enough to immerse a HOPG substrate. Hydrophobic HOPG was cleaved and immediately dipped into the sonicated dispersion. The stepper motor of the KSV 2000 was used to vertically withdraw the substrate from solution at a rate of 0.3 mm min^{-1}. Roughly 2 h were spent at this rate for the 2-D array coating a 10–12 mm vertical length of the substrate. All experiments were carried out at room temperature (23 ± 1 °C) and 45–55% relative humidity.

Electrochemical deposition

The electrochemical synthesis was carried out in a three-electrode cell using a potentiostat (Princeton Applied Research, Parstat 2263) to control the thickness of the polymerized materials. Working electrodes were prepared as PS latex beads array/HOPG substrates. A platinum wire and an Ag/Ag^+ electrode were used as counter and reference electrode, respectively. 0.05 M py with 0.05 M py–CHO was contained in 0.5 M potassium chloride (KCl) as supporting electrolyte. Constant potential (+0.65 V) was applied on the working electrode for various constant times.

Instrumentation

Atomic force microscopy (Agilent 5500 AFM/SPM System, Agilent Technologies) was used to investigate surface morphologies and surface analysis. The AFM measurements were carried out using a piezoscanner capable of scanning an area of ~10 × 10 μm^2 at room temperature. Commercially available tapping mode tips (TAP300, Silicon AFM Probes, TedPella, Inc.) were used on cantilevers with a resonance frequency in the range of 290–410 kHz. All images (AFM topography, Tapping mode) were filtered, and analyzed by using SPIP software (Scanning Probe Image Processor, Imagemet.com). Scanning electron microscopy (SEM, Gemini) was also used to investigate the surface morphology.

Results and discussion

Scheme 1 shows a summary of the fabrication method for highly ordered 2-D microporous films by using the LB-like technique and electrodeposition. Firstly, a colloidal monolayer consisting of (PS-m)s was transferred onto HOPG. After vacuum drying in an oven for several hours, the PS-m template on the HOPG was used as a working electrode in a three-electrode cell electrodeposition. A constant potential (potentiostatic method) was applied to a vertically aligned substrate for a specific time period, and then the electrodeposited film was rinsed with toluene to dissolve and remove the PS-m template. This process resulted in a highly ordered porous array film possessing various shapes and openings with precise control of the thickness under selective electrochemical conditions (*i.e.* primarily electrodeposition time).

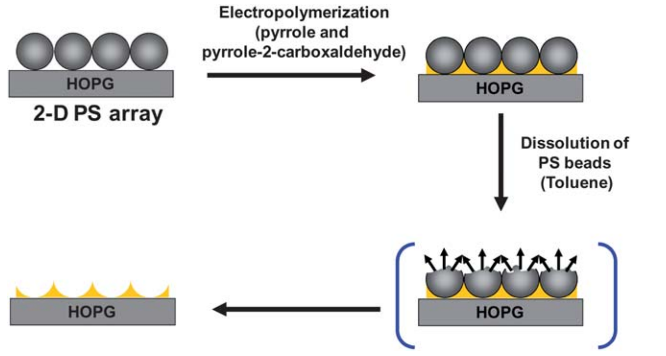

Scheme 1 Procedure involved in creating an asymmetrically functionalized microporous film consisting of Ppy/Ppy–CHO.

Commercially available (PS-m)s with a slight anionic charge from the sulfate ester are difficult to transfer as highly packed arrays using a conventional LB technique due to their high hydrophilicity and size. To overcome this limitation, several methods have been attempted and optimized as mentioned above. In particular, the PS-m arrays were formed with the aid of SDS as a spreading agent which assisted in single-layer formation at variable concentrations of the SDS.[15] From the atomic force microscope (AFM) and scanning electron microscope (SEM) images (Fig. 1), it is clear that the (PS-m)s transferred in a highly ordered manner on the HOPG substrate and that the array exhibited a hexagonally packed close structure. It should be noted that the structure can be controlled by the SDS concentration (above the critical micelle concentration—CMC) with the PS-m suspension. The addition of the SDS causes the migration of the PS-m from the bulk solution to the air–water interface. The PS-m is then transferred onto the hydrophobic HOPG by lateral attractive forces which then undergo reorganization on the substrate during evaporation of the liquid thin film near the meniscus.[15] Thus, it is possible to produce a highly ordered 2-D array of the PS-m on HOPG for the fabrication of microporous conducting polymeric films.

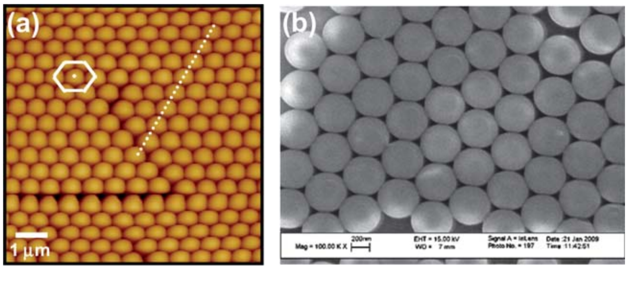

Fig. 1 (a) AFM and (b) SEM images of the hexagonal array template of the PS latex beads on the HOPG substrates by the LB-like technique.

In order to polymerize the electroactive pyrrole monomers and its aldehyde derivative (py–CHO) on the interstitial voids of the PS-m template, electrochemical deposition was performed at a constant potential of 0.65 V (*vs.* Ag/AgCl) for 250 s. After electrodeposition on the PS-m template, there is no significant or visible change on the surface morphology (AFM) due to the thin film growth on the voids and the short duration of electrochemical deposition. The PS-m template array was then removed by dissolving with toluene to reveal a well-ordered 2-D porous array on HOPG (d_{pore} = ~210 nm) with a constant distance (D_1 = ~155–160 nm) (Fig. 2a). The center-to-center distance (550 nm) between each pore is almost identical to the diameter of the PS-m.

The thickness of the thin Ppy/Ppy–CHO film was found to be ~25–26 nm (t_1), and a protruded ring around each pore was observed, with about 35–38 nm (t_2) in height. The thicker protrusion may result from the collapse of the irregularly grown film along the geometrically charged PS-m during electrodeposition (Fig. 2).[12a] In other words, the array structure of the charged PS-m template can affect the growth of the film. In Fig. 2b (SEM image) we found that the shape of each protruded portions on the microporous array is somewhat irregular and distorted with an average diameter of 330–350 nm; however, the porous sub-micron array remained hexagonally structured.

A longer electrodeposition time (350 s) led to thicker Ppy/Ppy–CHO film growth that extended beyond the interstitial voids. After the extraction of the template, various open shaped pores were observed as shown in Fig. 3. In all cases, the small concave triangular gaps or spandrels between each pore on the sub-microporous film were observed, resulting from a preferential polymer growth around the PS-m surface, presumably due to the effect of the charged surface. Nanosphere lithography (NSL) of

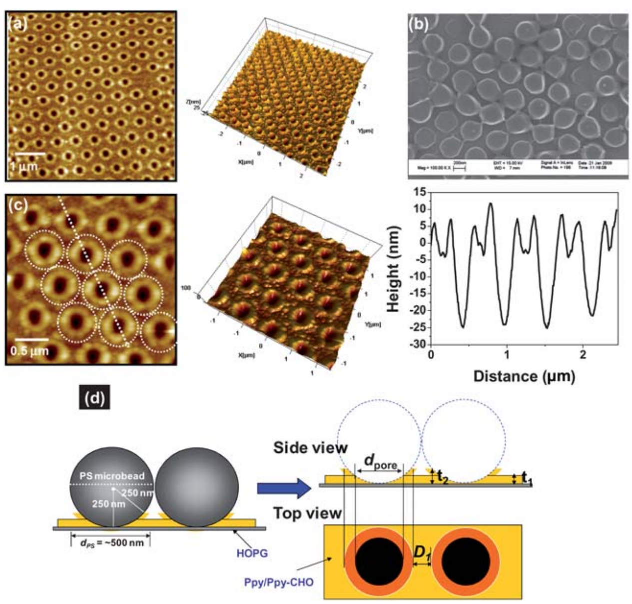

Fig. 2 (a) AFM (2-D and 3-D) and (b) SEM images of the hexagonal porous structured Ppy/Ppy–CHO polymeric film after electrochemical deposition in 0.5 M KCl and 50 mM py/50 mM py–CHO for 250 s and the extraction of the PS-m template, (c) zoom-in AFM image (2-D and 3-D) and line profilometry, and (d) dimension of the micropores array measured from the AFM image.

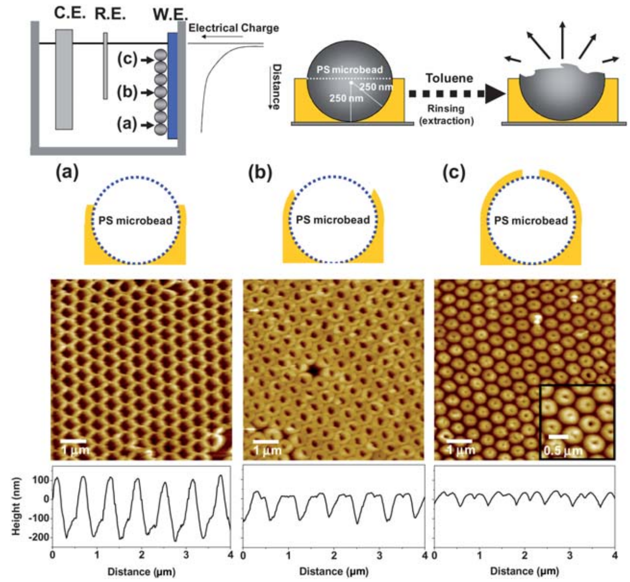

Fig. 3 Electrochemical setup, AFM images (a, b, and c), and corresponding line profilometries of the hexagonal porous structured Ppy/Ppy–CHO polymeric film after electrochemical deposition in 0.5 M KCl and 50 mM py/50 mM py–CHO for 350 s and the extraction of the PS-m template. (a), (b), and (c) are gradient of distance-dependent from the potential source.

metals and conductive polymers (*i.e.* polyaniline, polybithiophene, polypyrrole) has been similarly observed through electrochemical synthesis.[12b] In this case, there is a gradient electrical charge (field) along the vertical direction from the potential source (distance dependent) during electrodeposition, such that the thickness of the film was not constant over the entire sample area. This effect provides for various thicknesses on the polymeric film related to the different porous shapes observed. At a relatively low charged local area ("a" in Fig. 3), a honeycomb structure was formed as shown in the AFM image, where the film growth reached above the radius of the PS-m. The thickness of the film is ~300 nm and the hole is 425 nm in diameter. This morphology is very much similar to polymeric pores obtained from dissolution of polyelectrolyte (PE)-coated PS-m.[16] During extraction, rupturing forces may act in all directions out of the PS-m surface exposed to toluene. The extraction process on the hexagonally close-packed array did not impede the regularity of the porous array film produced. With higher charged electrode area (Fig. 3b), the film growth appears to be above the radius of the sphere template (>250 nm), and the opening size of the pore is significantly decreased due to the center-inward film growth along the upper half of the PS-m surface and collapse during the extraction which is similar to the formation of a dome from the ground up. From the line profilometry, flat periodic lines are shown on the collapsed portions, possessing flat ring-shaped structures.

Considering the collapsed upper portion of the film, this thickness is almost the same as in the case of the array in Fig. 3a. Comparison of the pore depth on the line profiles is somewhat inaccurate because the AFM tip cannot reach the bottom of the substrate through the narrow opening of the micropores during the scanning. However, the width and openings of the pores can be measured. Fig. 3c shows the sub-micropores obtained from the highest electrical charge examined. In this case, it appears that each pore is observed to have a regular pinhole on the center. A similar structure has been reported based on the surface morphology of a top layer on a 3-D porous structure obtained from polybithiophene.[12b] This structure consists of a hollow shell or dome like structure due to the "skin effect", forcing the porous polymeric materials not to shrink. From these three different results, it is possible to infer that the porous morphology and the regularity seen with the Ppy/Ppy–CHO film growth do not exceed the PS-m monolayer thickness, *i.e.* complete shielding or dome formation on the PS-m with the conductive polymer during electrodeposition (more than 500 s). There is a potential that such structures can be useful for dual patterning or dual chemical patterning in which the unfilled part of the electrode is still amenable for further electrochemistry or self-assembled monolayer modification (with Au or ITO electrodes).

From the SEM images (Fig. 4), we observed the similar opening shapes as the AFM images shown in Fig. 3a and b. In order to investigate the electrodeposited film on disordered and random arrays for comparison, we examined the edge region of the sample substrate.

These results clearly reveal that during electropolymerization, the presence of more than one type of single monomer flux towards the electrode occurs and is governed by the electrode geometry and proximity of the counter and reference electrodes.[17]

Considering the polymer growth at an applied potential, *V*, the current density at any point on a chronoamperogram (*i*) gives rise to a mass of flux density (*J*), which, according to Fick's law, creates a concentration gradient ($\partial c/\partial x$) with an assumed diffusion coefficient, *D*. The electric field variation for a single flux is given by:

$$\theta(x,\ t) = L\frac{\partial E \partial c}{\partial c \partial x}$$

where *L* and ($\partial E/\partial x$) are, respectively, the electrode length and the e-field gradient with the concentration. This simple relation should allow us to infer from the simultaneous occurrence of various fluxes in the electrode surface a gradient with a maximum value closer to where the position of the counter electrode (C.E.) and reference electrode (R.E.) is as shown in Fig. 3. Other experimental configurations can yet be optimized. Nevertheless, the geometry used in this experiment was sufficient to allow us to observe the various array morphologies. The field gradient effect has also been observed to affect the electrochemical synthetic mechanism for the formation of conductive polymer nanotubes in a porous anodized alumina template with poly(3,4-ethylenedioxythiophene) (PEDOT) as a function of monomer concentration and potential, therefore, electropolymerization leads either to solid nanowires or to hollow nanotubes.[18]

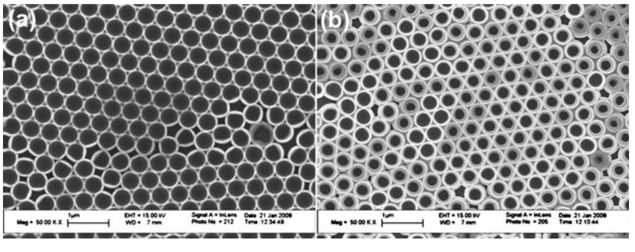

Fig. 4 SEM images (a and b) of two different opening shapes appeared on the same hexagonal porous structured Ppy/Ppy–CHO polymeric film after electrochemical deposition in 0.5 M KCl and 50 mM py/50 mM py–CHO for 350 s and the extraction of the PS-m template.

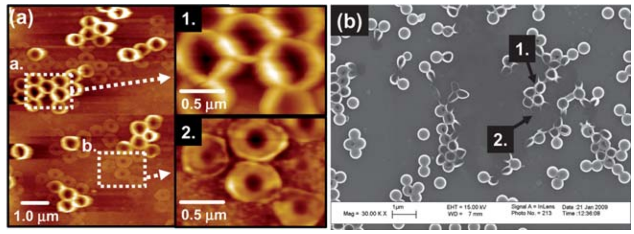

Fig. 5 (a) AFM and (b) SEM images on the edge of the film after electrochemical deposition in 0.5 M KCl and 50 mM py/50 mM py–CHO for 350 s and the extraction of the PS-m template.

In Fig. 5a, two distinct pore shapes were observed from the AFM images: (1) the hemisphere shells formed from partially the same geometric structure as the 2-D array and (2) widely opened thin pores obtained from the minor effect of a charged PS-m, with or without the reduced interstitial region with electrodeposition. SEM images were also investigated to obtain further insight on the surface morphology of the closed region. In regions 1 and 2 (Fig. 5b), similar pore shapes as shown in the AFM images were observed as well as hollow shells and shielded (PS-m)s. However, porous structures made from smaller PS microbeads (d_{ps} = 100 nm) retain only hemisphere shells (see Fig. S1, ESI†). It might be ascribed to the geometric stability and the extent of rigidity of the shells with the smaller pores during the extraction of the (PS-m)s.

The fact that these capsules and shells are observed to be unattached to the surface or not close packed indicates the potential of the method for hollow-shell particle fabrication. It is clear that there is a wide range of size, shape, and packing features that can be observed simply by controlling the gradient of the electric field. The electrodeposition time is only one of several electrochemical parameters that can be used to control pattern and particle formation. Efforts can be made to observe and optimize other parameters, *e.g.* concentration, solvent, supporting electrolytes, electrode geometry, *etc.* in both potentiostatic and potentiodynamic conditions. Variation on the size of the template particle or the composition of the polymer is obvious, *e.g.* other conducting polymers such as polyaniline, polythiophene, *etc.* Finally we suggest that the porous film with the right functional groups can be applicable for a biosensing system, an example of which is *via* molecular imprinting system using protein functionalized polystyrene beads. The fact that the Ppy–CHO has an aldehyde group makes it amenable for bio-conjugation chemistry. The various sizes and shapes that can be produced would result in various surface areas and geometries—for binding or detection of analytes. It is also of high interest as a "toolbox" for various shapes or patterns that can be combined with other non-lithographic patterning methods. These studies are currently underway.

Conclusions

In conclusion, we have demonstrated the formation of highly ordered 2-D sub-microporous conducting polymeric arrays fabricated by an LB-like technique and electrodeposition method on HOPG. The emphasis is on singe-layer templating *versus* 3-D inverse opal generation. The morphology, size, and shape can be varied depending on the time duration of electrodeposition. Furthermore, the current density (e-field gradient) enables various porous opening shapes to be made on the same substrate such as honeycomb, flat ring-shape, and hollow shell structures. The system can also be utilized towards the formation of a specific shape, size, packing structure, and composition of feature depending on the parameterization above.

Acknowledgements

The authors gratefully acknowledge partial funding from the National Science Foundation, DMR-10-06776, CBET-0854979, and Robert A Welch Foundation, E-1551. We also acknowledge technical support from Agilent Technologies.

References

1 Y. Xia, B. Gates, Y. Yin and Y. Lu, *Adv. Mater.*, 2000, **12**, 693.
2 Y.-H. Ye, F. Leblanc, A. Haché and V.-V. Truong, *Appl. Phys. Lett.*, 2001, **78**, 52.
3 B. Varghese, F. C. Cheong, S. Sindu, T. Yu, C.-T. Lim, S. Valiyaveettil and C.-H. Sow, *Langmuir*, 2006, **22**, 8248.
4 (*a*) M. Trau, D. Saville and I. Aksay, *Science*, 1996, **272**, 706; (*b*) S. Yeh, M. Seul and B. Shraiman, *Nature*, 1997, **386**, 57; (*c*) Y. Solomentsev, M. Böhmer and J. Anderson, *Langmuir*, 1997, **13**, 6058; (*d*) G. Picard, I. Nevernov, D. Alliata and L. Pazdernik, *Langmuir*, 1997, **13**, 264.
5 (*a*) Y.-H. Ye, S. Badilescu, V.-V. Truong, P. Rochon and A. Natansohn, *Appl. Phys. Lett.*, 2001, **79**, 872; (*b*) V. Kitaev and G. A. Ozin, *Adv. Mater.*, 2003, **15**, 75.
6 F. Burmeister, C. Schäfle, T. Matthes, M. Böhmisch, J. Boneberg and P. Leiderer, *Langmuir*, 1997, **13**, 2983.
7 (*a*) Y. Yin, Y. Lu, B. Gates and Y. Xia, *J. Am. Chem. Soc.*, 2001, **123**, 8718; (*b*) Y. Yin, Y. Lu and Y. Xia, *J. Am. Chem. Soc.*, 2001, **123**, 771.
8 (*a*) B. van Duffel, R. H. A. Ras, F. C. De Schryver and R. A. Schoonheydt, *J. Mater. Chem.*, 2001, **11**, 3333; (*b*) S. Huang, K. Minami, H. Sakaue, S. Shingubara and T. Takahagi, *Langmuir*, 2004, **20**, 2274; (*c*) M. Szekeres, O. Kamalin, R. A. Schoonheydt, K. Wostyn, K. Clays, A. Persoons and I. Dékány, *J. Mater. Chem.*, 2002, **12**, 3268; (*d*) Z.-C. Lü, W.-D. Ruan, N. Ji, L.-Q. Ren, Q. Cong and B. Zhao, *J. Bionic Eng.*, 2006, **3**, 59.
9 Y. J. Zhang, W. Li and K. J. Chen, *J. Alloys Compd.*, 2008, **450**, 512.
10 P. V. Braun and P. Wiltzius, *Nature*, 1999, **402**, 603.
11 P. N. Bartlett, J. J. Baumberg, S. Coyleb and M. E. Abdelsalam, *Faraday Discuss.*, 2004, **125**, 117.
12 (*a*) F. Sun, W. Cai, Y. Li, B. Cao, F. Lu, G. Duan and L. Zhang, *Adv. Mater.*, 2004, **16**, 1116; (*b*) P. N. Bartlett, P. R. Birkin, M. A. Ghanem and C.-S. Toh, *J. Mater. Chem.*, 2001, **11**, 849.
13 T. Sumida, Y. Wada, T. Kitamura and S. Yanagida, *Chem. Commun.*, 2000, 1613.
14 R. Eggins, *Biosensor: An Introduction*, Wiley & Teubner, 1996, pp. 31–50.
15 M. Marquez and B. P. Grady, *Langmuir*, 2004, **20**, 10998.
16 S. Han, A. L. Briceño, X. Shi, D. A. Mah and F. Zhou, *J. Phys. Chem. B*, 2002, **106**, 6465.
17 L. M. Abrantes and J. P. Correia, *Electrochim. Acta*, 1999, **44**, 1901.
18 R. Xiao, S. Cho, R. Liu and S. B. Lee, *J. Am. Chem. Soc.*, 2007, **129**, 4483.